Conformal Strip Excitation of Dielectric Resonator Antenna

Kwok Wa Leung, *Member, IEEE*

***Abstract*—In this paper, a new excitation scheme that employs a conducting conformal strip is proposed for dielectric resonator antenna (DRA) excitation. The new excitation scheme is successfully demonstrated by using a hemispherical DRA whose exact Green function is found using the mode-matching method. The moment method is used to solve the unknown strip current from which the input impedance is obtained. Novel recurrence formulas were obtained so that the impedance integrals are evaluated analytically. This solves the singularity problem of the Green function and substantially reduces the computation time. An experiment was carried out to verify the theory. The co- and cross-polarized field patterns are also shown in this paper. In addition, an experimental technique which deals with the problem of an air gap between the DRA and the ground plane is presented.**

***Index Terms*—Dielectric resonator antennas.**

I. INTRODUCTION

BECAUSE of having no metallic loss, the dielectric resonator antenna (DRA) [1] is potentially attractive for millimeter-wave applications. Other advantages of the DRA are small size, light weight, low cost, and ease of excitation. For these reasons, the DRA has been studied extensively [2]–[24] since the work reported by Long *et al.*. [1].

A number of excitation methods have been investigated, such as the coaxial-probe feed [1]–[7], aperture-coupling feed [8]–[13], direct microstripline feed [14], [15], coplanar waveguide feed [16], soldered-through probe [17], and, more recently, perpendicular feed [18], [19]. Among the various excitation methods, the coaxial-probe feed was first used to demonstrate the radiation capability of the DRA [1]. In this method, a hole was drilled inside the DRA for the probe penetration. However, two practical problems arise when using this method. First, drilling a hole in a super-hard DR is rather difficult. Second, it is almost impossible to have a hole that perfectly fits the size of the probe and, usually, an air gap exists between the probe and the DRA. This causes the measured results to deviate from the theoretical design [4], [20]. Although other excitation methods [8]–[16] can be used to avoid these problems, the probe-feed method is still preferred in some applications. For example, it is simpler and more direct to use a coaxial probe to excite the DRA residing on the rooftop of a vehicle. Moreover, the probe-feed method admits easy excitation of circularly polarized fields by simply adding a 90° displaced probe in phase quadrature [21], [22]. To avoid the drilling-hole problem the probes in [21], [22] were placed outside the DRA. This approach is feasible only when the DRA has a vertical side wall such as cylindrical and rectangular DRAs. For DRAs with a curved side wall (e.g., hemisphere and half-split cylinder [12]), however, the coupling between the probe and DRA is rather inefficient. To overcome this problem, a new excitation scheme which employs a conformal conducting strip is proposed. In this method, the strip is mounted on the surface of a DRA, as shown in Fig. 1. The new method possesses the same advantage of the coaxial-probe feed. On the other hand, it allows the whole electric current to flow on the DRA surface and, thus, is more efficient in energy coupling than the probe-feed counterpart [21], [22]. Furthermore, the new method can be easily implemented by just cutting a strip from an adhesive conducting tape. As compared with the traditional probe-feed method [1]–[7], the new method desirably avoids the problems of drilling a hole for the probe accommodation. Moreover, it allows very convenient post manufacturing trimmings because the conformal strip can be cut shorter without leaving an air gap or extended longer without the need for deepening the hole. It should be mentioned that by using a soldered-through probe [17] the new excitation scheme can also be integrated with millimeter-wave integrated circuits (MMICs).

For ease of analysis, the hemispherical DRA, excited at the fundamental broadside TE_{111} mode is chosen to demonstrate the new excitation method. Nevertheless, the feed method can be applied to other DRAs. In this paper, the mode-matching method [4] is used to obtain the exact Green function of the hemispherical DRA. First the electric and magnetic potential Green functions inside and outside the DRA are found by matching the boundary conditions at the DRA-air interface. From the potential Green functions, the fields inside and outside the DRA are obtained readily [25]. Then an integral equation for the strip current is formulated, which is solved using the moment method. In evaluating the impedance elements, it is difficult to perform the numerical integration due to the singularity problem of the DRA Green function. To solve this problem, the integration is performed analytically by virtue of novel recurrence formulas. Since the final result is a regular modal series, it can be easily computed in a straightforward manner. The modal solution consists of two summations. Theoretically, one of them has an infinite number of terms, but it was found that the summation can be truncated to about 65 terms for the fundamental TE_{111} mode. In addition to the fact that the result involves no numerical integration, the solution is computationally very efficient.

Manuscript received August 27, 1998; revised April 4, 2000. This work was supported by a Strategic Research Grant, Project 7 000 928, City University of Hong Kong, and by an RGC Earmarked Research Grant Project 9 040 209.

The author is with the Department of Electronic Engineering, City University of Hong Kong, Kowloon, Hong Kong (email: eekleung@cityu.edu.hk).

Publisher Item Identifier S 0018-926X(00)05790-2.

0018–926X/00$10.00 © 2000 IEEE

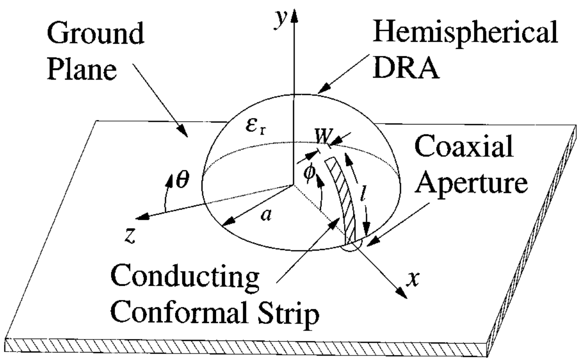

Fig. 1. The configuration of the conformal strip-fed DRA.

In DRA measurements, it is inevitable to have an air gap between the DRA and the ground plane, causing a discrepancy between theory and experiment. To solve this problem, Junker *et al.* [20] used a section of PVC pipe, which contained a powdered dielectric material for their DRA measurements. In this paper, a new technique that suits a solid DRA is presented to tackle the problem, and significant improvement was found in the impedance measurement.

In this paper, the effects of the strip length and dielectric constant on the input impedance are studied. Moreover, the co- and cross-polarized field patterns are presented. It is found that the new configuration has a much weaker cross-polarized field than the previous probe-feed version, as desired.

II. FORMULATION

A perspective view of the configuration is shown in Fig. 1, where a hemispherical DRA of radius a and dielectric constant ε_r is fed by a conformal strip of length l and width W. To begin with, image theory is used so that an equivalent problem of a strip of total length $2l$ mounting on a spherical DRA is obtained. The input impedance of the original problem is then one-half that of the new one [4]. For convenience, the coordinate system shown in Fig. 1 is chosen for the analysis. Fig. 2 shows the x-y and x-z planes of the equivalent configuration. The conformal strip subtends the azimuthal and elevation angles from $-\phi_1$ to ϕ_1 (Fig. 2(a)) and θ_1 to $\pi-\theta_1$ (Fig. 2(b)), respectively. In the following formulation, the time dependence $e^{j\omega t}$ is used which is suppressed. The field and source points are denoted by $\vec{r}(r,\theta,\phi)$ and $\vec{r}'(r',\theta',\phi')$, respectively. Using the mode-matching method, the Green function ($r=r'=a$) of E_ϕ due to a ϕ-directed point current is found as follows:

$$\begin{aligned} G = &\frac{j\eta_0}{4\pi a^2}\sum_{n=1}^{\infty}\sum_{m=0}^{n}\frac{2n+1}{n(n+1)\Delta_n^{\mathrm{TE}}}\hat{J}_n(ka)\hat{H}_n^{(2)}(k_0a)\\ &\cdot\frac{2}{\Delta_m}\cdot\frac{(n-m)!}{(n+m)!}\cdot\frac{dP_n^m(\cos\theta)}{d\theta}\\ &\cdot\frac{dP_n^m(\cos\theta')}{d\theta'}\cos m(\phi-\phi')\\ &-\frac{j\eta_0}{4\pi a^2}\sum_{n=1}^{\infty}\sum_{m=1}^{n}\frac{2n+1}{n(n+1)\Delta_n^{\mathrm{TM}}}\hat{J}_n'(ka)\hat{H}_n^{(2)\prime}(k_0a)\\ &\cdot 2m^2\cdot\frac{(n-m)!}{(n+m)!}\cdot\frac{P_n^m(\cos\theta)}{\sin\theta}\\ &\cdot\frac{P_n^m(\cos\theta')}{\sin\theta'}\cos m(\phi-\phi') \end{aligned}\tag{1}$$

where

$$\Delta_n^{\mathrm{TE}} = \hat{J}_n(ka)\hat{H}_n^{(2)\prime}(k_0a) - \frac{k}{k_0}\hat{J}_n'(ka)\hat{H}_n^{(2)}(k_0a) \tag{2}$$

$$\Delta_n^{\mathrm{TM}} = \hat{J}_n'(ka)\hat{H}_n^{(2)}(k_0a) - \frac{k}{k_0}\hat{J}_n(ka)\hat{H}_n^{(2)\prime}(k_0a) \tag{3}$$

$$\Delta_m = \begin{cases}1, & m>0\\ 2, & m=0\end{cases} \tag{4}$$

and η_0 is the wave impedance in vacuum. In (1)–(3), $P_n^m(x)$ is the associated Legendre function of the first kind of order m and degree n, and $\hat{J}_n(x)$ and $\hat{H}_n^{(2)}(x)$ are nth order Schelkunoff-type ([25], p. 268) spherical Bessel and Hankel functions. All other symbols have the usual meanings. A prime denotes a derivative with respect to the whole argument. It should be mentioned that the double-summations of the Green function can be reduced to single-summations by using the addition theorem for Legendre polynomials. This technique has been used elsewhere [4], [9], [26] to simplify the expressions and to reduce the computation time. In this paper, however, the double-summations are retained in the Green function to allow analytical treatments for impedance calculations, as will be seen shortly.

Define E_ϕ^s and E_ϕ^i as the scattered and impressed fields due to the current density $J_{\phi s}$ and the excitation source, respectively. Then by enforcing the boundary condition that the total tangential electric field vanishes on the (conducting) strip surface, we have

$$E_\phi^s + E_\phi^i = 0 \tag{5}$$

or

$$-\iint_{S_0} G(\theta,\phi;\theta',\phi')J_{\phi s}(\phi')\,dS' = E_\phi^i \tag{6}$$

where S_0 is the surface of the conformal strip. The delta gap source model is used so that the impressed field E_ϕ^i can simply be written as $(V_0/a)\delta(\phi)$, where V_0 is the voltage amplitude at the feed point. Let $I(\phi)=J_{\phi s}W$ be the strip current, then (6) becomes

$$\frac{-1}{W}\iint_{S_0} G(\theta,\phi;\theta',\phi')I(\phi')\,dS' = \frac{V_0}{a}\delta(\phi). \tag{7}$$

The moment method is employed to expand the unknown strip current as $I(\phi)=\sum_{q=1}^{N}I_q f_q(\phi)$, where $f_q(\phi)$ are piecewise sinusoidal (PWS) basis functions given by $f_q(\phi)=[\sin k_e(h-a|\phi-\phi_q|)]/\sin k_e h$ for $a|\phi-\phi_q|<h$ and $f_q(\phi)=0$, otherwise, with $h=2l/(N+1), \phi_q=(-l+qh)/a$ and $k_e=\sqrt{(\varepsilon_r+1)/2}k_0$ being the PWS mode half-length, the center point of the qth expansion mode, and the effective wavenumber

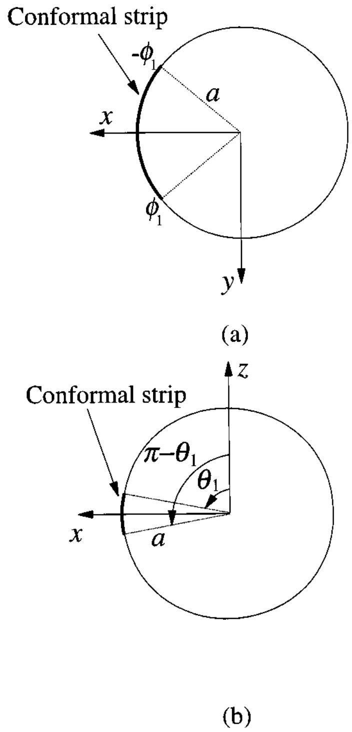

Fig. 2. The angles subtended by the strip of the equivalent configuration. (a) x–y plane. (b) x—z plane.

at the DRA-air interface, respectively. I_q are unknown coefficients to be determined. Following the procedure of [26], the following matrix equation is obtained:

$$\lfloor Z_{pq} \rfloor \lfloor I_q \rfloor = \lfloor f_p(0) \rfloor \tag{8}$$

where

$$Z_{pq} = \frac{-1}{W^2} \iint_{S_0} \iint_{S_0} f_p(\phi) G(\theta, \phi; \theta', \phi') f_q(\phi')\, dS'\, dS. \tag{9}$$

Once I_q are obtained, the input impedance is easily found from $Z_{\text{in}} = 1/\sum_{q=1}^{N} I_q f_q(0)$. Finally, dividing Z_{in} by two gives the input impedance of the original problem. In the next section, analytical treatments for Z_{pq} are carried out so that the solution can be calculated very easily and efficiently.

III. Evaluation of Z_{pq}

The impedance matrix elements Z_{pq} of (9) cannot be integrated numerically. This is because $G(\theta, \phi; \theta', \phi')$ is a singular Green function as $\vec{r} \rightarrow \vec{r}'$ and, thus, an excessive number of modal terms is required to calculate $G(\theta, \phi; \theta', \phi')$ accurately. However, the amplitudes of higher order Hankel functions are so high that they are difficult to handle numerically. Moreover, considerable computation time is required if a large number of terms are included in the solution. To solve these problems, the quadruple integration is performed analytically using novel recurrence formulas. Since the final result does not involve any singularity, it can be implemented in a straightforward manner. First note that (9) can be written as

$$\begin{aligned} Z_{pq} = \frac{-ja^2\eta_0}{4\pi W^2} \sum_{n=1}^{\infty} \frac{2n+1}{n(n+1)} \Bigg\{ & \frac{\hat{J}_n(ka)\hat{H}_n^{(2)}(k_0 a)}{\Delta_n^{\text{TE}}} \\ & \times \sum_{m=0}^{n} \frac{2}{\Delta_m} \cdot \frac{(n-m)!}{(n+m)!} [\Theta_1(n,m)]^2 \Phi_1(p,q,m) \\ & - \frac{\hat{J}_n'(ka)\hat{H}_n^{(2)\prime}(k_0 a)}{\Delta_n^{\text{TM}}} \sum_{m=1}^{n} 2m^2 \\ & \cdot \frac{(n-m)!}{(n+m)!} [\Theta_2(n,m)]^2 \Phi_1(p,q,m) \Bigg\} \end{aligned} \tag{10}$$

where

$$\Theta_1(n,m) = \int_{\theta_1}^{\pi-\theta_1} \frac{dP_n^m(\cos\theta)}{d\theta} \sin\theta\, d\theta \tag{11}$$

$$\Theta_2(n,m) = \int_{\theta_1}^{\pi-\theta_1} P_n^m(\cos\theta)\, d\theta \tag{12}$$

$$\begin{aligned} \Phi_1(p,q,m) = \int_{\phi=\phi_p-\phi_h}^{\phi_p+\phi_h} \int_{\phi'=\phi_q-\phi_h}^{\phi_q+\phi_h} & f_p(\phi) \\ & \times \cos m(\phi - \phi') f_q(\phi')\, d\phi'\, d\phi \end{aligned} \tag{13}$$

in which $\phi_h = h/a$. The integral $\Theta_2(n,m)$ is considered first. To calculate $\Theta_2(n,m)$ efficiently, two novel recurrence formulas were derived. The first one is recursive in n and is given by

$$\begin{aligned} \Theta_2(n+1,m) = & \frac{1}{(n+1)(n-m+1)} \\ & \times \Big\{ -(2n+1)[1-(-1)^{n+m}] \sqrt{1-x_1^2} P_n^m(x_1) \\ & + n(n+m)\Theta_2(n-1,m) \Big\} \end{aligned} \tag{14}$$

where $x_1 = \cos\theta_1$. The initial values for $m = 0$ are given by $\Theta_2(0,0) = 2\sin^{-1} x_1$ and $\Theta_2(1,0) = 0$. From the initial values all $\Theta_2(n,0)$ can be found easily. After $\Theta_2(n,0)$ are obtained, $\Theta_2(n,m)$ can be calculated using another formula, which is recursive in m

$$\begin{aligned} \Theta_2(n,m+2) = & -2\lfloor 1+(-1)^{n+m} \rfloor P_n^{m+1}(x_1) \\ & + (n+m+1)(n-m)\Theta_2(n,m) \end{aligned} \tag{15}$$

and the initial values are $\Theta_2(n,0)$ and $\Theta_2(n,1) = [(-1)^n - 1]P_n(x_1)$.

Next, the integral $\Theta_1(n,m)$ is considered. For a slender strip we have $\theta_1 \approx \pi/2$ and $x_1 \approx 0$. By using this approximation, the following simple expression for $\Theta_1(n,m)$ is obtained:

$$\Theta_1(n,m) \approx [(-1)^{n+m} - 1] P_n^m(x_1). \tag{16}$$

It should be mentioned that (16) is exact when $n+m$ is even, at which $\Theta_1(n,m) = 0$. In this paper, however, an exact formula is used to calculate $\Theta_1(n,m)$ for all n and m. The formula makes use of $\Theta_2(n,m)$ and is given by

$$\Theta_1(n,m) = [(-1)^{n+m}-1]\sqrt{1-x_1^2}P_n^m(x_1) - \frac{1}{2n+1}[(n+m) \times \Theta_2(n-1,m) - (m-n-1)\Theta_2(n+1,m)]. \quad (17)$$

The last integral $\Phi_1(p,q,m)$ can be integrated analytically. The result consists of 64 terms and is expressed in the following compact form:

$$\Phi_1(p,q,m) = \frac{1}{\sin^2 k_e h}\sum_{i'=-1,1}\sum_{j'=-1,1}\sum_{l'=-1,1}\sum_{i=-1,1}\sum_{j=-1,1}\sum_{l=-1,1} \times \frac{ll'\cos\lfloor i\alpha(l) - i'\alpha(l') - m(\phi_p-\phi_q)\rfloor}{4(k_e a + j'm)(k_e a + jm)} \quad (18)$$

where $\alpha(-1) = k_e h$ and $\alpha(1) = m\phi_h$. Note that the compact form (18) is very convenient for numerical programming. To this end, the impedance elements Z_{pq} can be calculated without the need for any numerical integration. Moreover, since x_1 is a simple constant, the values of $P_n^m(x_1)$ for all n and m are needed to be determined only once in one batch, with the results stored in an array. Similarly, the spherical Bessel and Hankel functions are needed to be calculated only once. Therefore, the computation time is extremely short. The convergence of the solution will be discussed in Section V.

IV. Radiation Fields

After the strip current is solved, the radiation fields E_θ and E_ϕ are obtained easily. The results are summarized here

$$E_\theta(r,\theta,\phi) = \frac{-\eta_0 a}{4\pi W}\cdot\frac{e^{-jk_0 r}}{r}\sum_{q=1}^{N} I_q E_{\theta q}(\theta,\phi) \quad (19)$$

$$E_\phi(r,\theta,\phi) = \frac{-\eta_0 a}{4\pi W}\cdot\frac{e^{-jk_0 r}}{r}\sum_{q=1}^{N} I_q E_{\phi q}(\theta,\phi) \quad (20)$$

where

$$E_{\theta q}(\theta,\phi) = \sum_{n=1}^{\infty} j^n \frac{2n+1}{n(n+1)}\left\{ j\frac{\hat{J}_n'(ka)}{\Delta_n^{\mathrm{TM}}}\sum_{m=1}^{n} 2m\cdot\frac{(n-m)!}{(n+m)!} \cdot\frac{dP_n^m(\cos\theta)}{d\theta}\Theta_2(n,m)\Phi_2(\phi,q,m) + \frac{\hat{J}_n(ka)}{\Delta_n^{\mathrm{TE}}}\sum_{m=1}^{n} 2m\cdot\frac{(n-m)!}{(n+m)!} \cdot\frac{P_n^m(\cos\theta)}{\sin\theta}\Theta_1(n,m)\Phi_2(\phi,q,m)\right\} \quad (21)$$

$$E_{\phi q}(\theta,\phi) = \sum_{n=1}^{\infty} j^n \frac{2n+1}{n(n+1)}\left\{ j\frac{\hat{J}_n'(ka)}{\Delta_n^{\mathrm{TM}}}\sum_{m=1}^{n} 2m^2\cdot\frac{(n-m)!}{(n+m)!} \cdot\frac{P_n^m(\cos\theta)}{\sin\theta}\Theta_2(n,m)\Phi_3(\phi,q,m) + \frac{\hat{J}_n(ka)}{\Delta_n^{\mathrm{TE}}}\sum_{m=0}^{n} \frac{2}{\Delta_m}\cdot\frac{(n-m)!}{(n+m)!} \cdot\frac{dP_n^m(\cos\theta)}{d\theta}\Theta_1(n,m)\Phi_3(\phi,q,m)\right\} \quad (22)$$

in which

$$\Phi_2(\phi,q,m) = \frac{1}{\sin k_e h}\sum_{i'=-1,1}\sum_{j'=-1,1}\sum_{l'=-1,1} \times\frac{l'\sin\lfloor m(\phi-\phi_q) + i'\alpha(l')\rfloor}{2(k_e a + j'm)} \quad (23)$$

$$\Phi_3(\phi,q,m) = \frac{1}{\sin k_e h}\sum_{i'=-1,1}\sum_{j'=-1,1}\sum_{l'=-1,1} \times\frac{l'\cos\lfloor m(\phi-\phi_q) + i'\alpha(l')\rfloor}{2(k_e a + j'm)}. \quad (24)$$

In deriving the radiation fields, we have used the asymptotic expressions $\hat{H}_n^{(2)}(k_0 r) \sim j^{n+1}e^{-jk_0 r}$ and $\hat{H}_n^{(2)\prime}(k_0 r) \sim j^n e^{-jk_0 r}$ for $r\to\infty$. Note that the magnetic far fields H_θ and H_ϕ can be easily found using $\vec{H} = (1/\eta_0)\hat{r}\times\vec{E}$.

V. Measured and Calculated Results

First the convergence of the modal solution (10) is discussed. Since the summation of index m has only a finite number of terms $(0 \le m \le n)$, we will focus on the summation of index n only. As is well known, the convergence rate of the solution depends on the arguments of the Bessel and Hankel functions. Since we are only concerned with the fundamental TE_{111} mode, it is informative to know the value of $\mathrm{Re}(ka)$, where ka is the first complex root of $\Delta_1^{\mathrm{TE}} = 0$ (Δ_1^{TE} is given in (2)). The result as a function of ε_r is shown in Fig. 3 for $3 \le \varepsilon_r \le 200$. It is observed that the value of $\mathrm{Re}(ka)$ increases very slowly with ε_r and $\mathrm{Re}(ka) \sim 3$. Therefore, the required number of terms should vary only slightly for different hemispherical DRAs operating at the mode. Also shown in Fig. 3 is the required number of modal terms for the solution to converge, with parameters $a = 12.5$ mm, $\varepsilon_r = 9.5, l = 12.0$ mm, and $W = 1.2$ mm. The results were calculated at $N = 3$ in the moment method and at frequencies $f = c\cdot\mathrm{Re}(ka)/(2\pi a\sqrt{\varepsilon_r})$, where c is the speed of light in vacuum. The convergence was checked by using the rule $|[Z_{\mathrm{in}}(\mathrm{new}) - Z_{\mathrm{in}}(\mathrm{old})]/Z_{\mathrm{in}}(\mathrm{new})| \le 10^{-4}$. With reference to the figure, the solution converges in 64–68 terms over the range of ε_r. It is interesting to note that the required number of terms does not change monotonically with $\mathrm{Re}(ka)$, as the solution involves $k_0 a$ as well. However, if the dielectric constant ε_r is fixed, the required number of terms should increase montonically with a and, thus, ka. Fig. 4 shows the convergence check using different numbers of modal terms. It is observed that the result converges in about 60 terms, as the result using 60 terms coincides with that using 80 terms. The result is very consistent with that of Fig. 3.

The calculation of the solution was found to be extremely fast. To see this, the computation time of the present theory is compared with that of the previous probe-feed solution [4]. As similar to the present theory, the delta gap source model and three

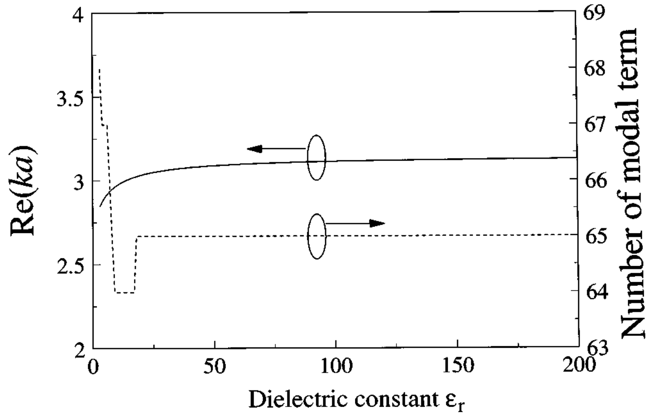

Fig. 3. The left axis shows the real part of the first root of the equation $\Delta_1^{\mathrm{TE}} = 0$. The right axis shows the number of terms required for the solution to converge. The parameters are $a = 12.5$ mm, $\varepsilon_r = 9.5, l = 12.0$ mm, and $W = 1.2$ mm.

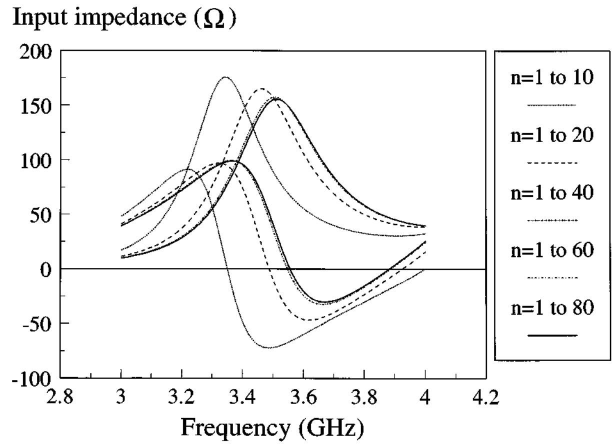

Fig. 4. The convergence check of the solution: $a = 12.5$ mm, $\varepsilon_r = 9.5, l = 12.0$ mm, and $W = 1.2$ mm.

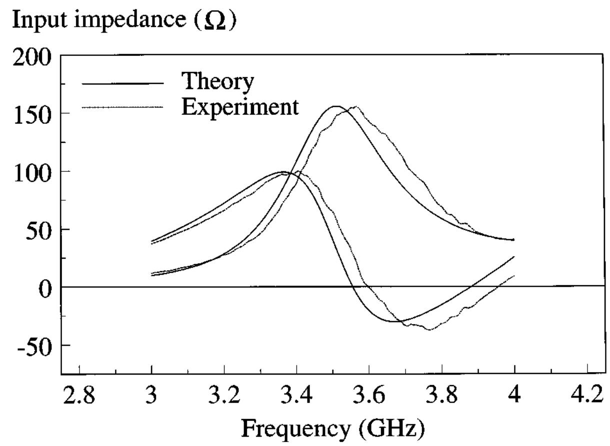

Fig. 5. Measured and calculated input impedances of the conformal strip-fed hemispherical DRA: $a = 12.5$ mm, $\varepsilon_r = 9.5, l = 12.0$ mm, and $W = 1.2$ mm.

PWS expansion modes were used in the previous probe-feed solution. The programs were run on a SunSPARC 20 Model 612 workstation. It was found that the average computation time for each frequency point were 0.15 and 2.07 sec for the present and previous solutions, respectively. The longer computation time in the previous solution is attributed to the numerical integration of the homogeneous solution (a formula had been used for the particular solution part [4]).

To verify the theory, an experiment was carried out using a hemispherical DRA of $a = 12.5$ mm and $\varepsilon_r = 9.5$. A conducting strip of length $l = 12$ mm and $W = 1.2$ mm was cut from an adhesive conducting tape. The measurement was performed using an HP8510C network analyzer, with the reference plane set at the coaxial aperture using the port extension. Originally, the DRA was simply put on an aluminum ground plane of size 30 × 30 cm. However, due to the surface roughness of the aluminum plate, an air gap existed between the DRA and the ground plane [20], causing the measured resonant frequency to have an error of more than 4%. To tackle this problem, the DRA was first put on the adhesive side of a conducting tape. Since the conducting tape is adhered to the base of the DRA conformally, the air gap was removed (to avoid the strip from shorting to the ground plane, there was no adhesive tape around the feed point and a very small air gap still existed). The size of the conducting tape was larger than the base of the DRA and additional adhesive tapes were used to mount the edges of the DRA-attached tape on the ground plane. Fig. 5 shows the measured and calculated input impedances of the DRA. Good agreement between theory and experiment is obtained. The discrepancy is caused by the small air gap round the feed point and by experimental tolerances. With reference to the figure, the measured and calculated resonant frequencies (zero reactance) are 3.60 and 3.56 GHz, respectively. The error is 1.1%, which is much smaller than the case without using the conducting adhesive tapes. This experimental technique was also used in [19] and, again, good result was obtained.

Fig. 6 shows the calculated input impedance for different strip lengths. As can be observed from the figure, the strip length can be adjusted to achieve impedance matching in practical designs. The results are similar to those in the probe-feed case [4].

Fig. 7 shows the calculated input impedance for different dielectric constants. Again, the results are similar to those in the probe-feed case; the higher the dielectric constant, the lower the resonant frequency and the narrower the bandwidth, as expected. It is observed that the reactance is shifted upward in the $\varepsilon_r = 5$ case. This is because when the dielectric constant is small, the modal fields of the DRA become relatively weak and are strongly influenced by the strip-monopole mode. In this case, the DRA will give a stronger cross-polarized field [23] and the design engineer should pay attention to this.

Fig. 8 shows the calculated E-plane (x-y plane in Fig. 1) and H-plane (y-z plane in Fig. 1) radiation field patterns at resonance ($f = 3.56$ GHz). The fields are of the broadside mode, as expected. It is observed that the maximum H-plane crosspolarized field is 24 dB lower than the maximum copolarized fields, whereas it was only 6 dB in the probe-feed version [24]. The difference is mainly caused by the fact that the conformal strip current does not have any J_r components whereas J_r components existed in the probe-feed case. The J_r components only

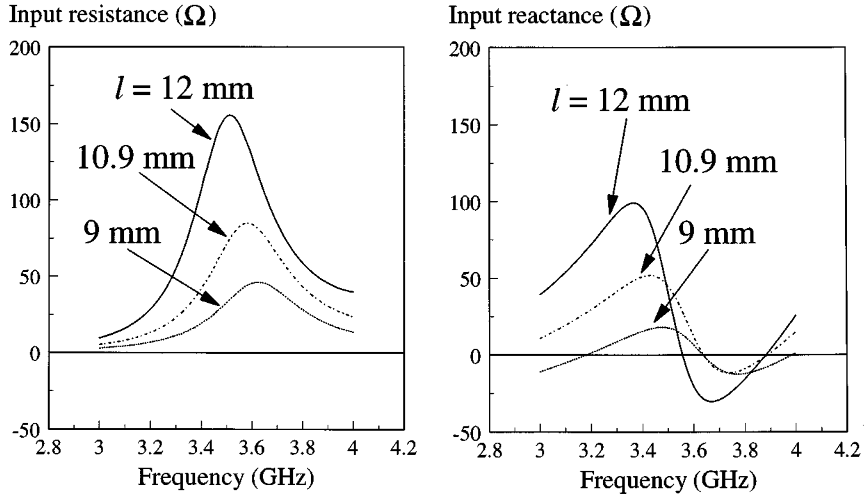

Fig. 6. Calculated input impedance of the DRA for different strip lengths: $a = 12.5$ mm, $\varepsilon_r = 9.5$, and $W = 1.2$ mm.

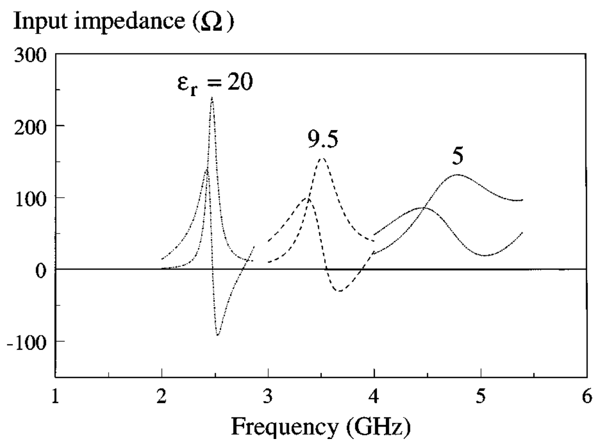

Fig. 7. Calculated input impedance of the DRA for different dielectric constants: $a = 12.5$ mm, $l = 12.0$ mm, and $W = 1.2$ mm.

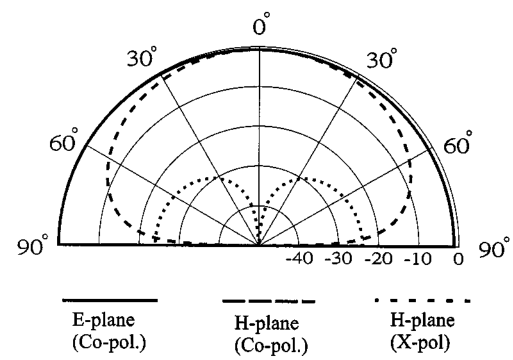

Fig. 8. Calculated co- and cross-polarized field patterns: $a = 12.5$ mm, $l = 12.0$ mm, $\varepsilon_r = 9.5$, and $W = 1.2$ mm.

excite TM modes, which entirely contribute to the crosspolarized field. For the E-plane crosspolarized field, it is theoretically zero and is omitted in the figure.

VI. Conclusion

The use of a conducting conformal strip for DRA excitation has been proposed. This excitation scheme shares the same advantage of a coaxial probe, but the effort in drilling a hole for the probe penetration and the errors that an oversized hole introduces will be avoided.

The new excitation scheme has been successfully demonstrated by using a hemispherical DRA, which is excited at the fundamental broadside TE_{111} mode. In the analysis, the mode-matching method has been used to obtain the exact Green function of the hemispherical DRA and the moment method has been employed to solve the unknown strip current. To avoid the singularity problem of the Green function, the impedance integral has been evaluated analytically by virtue of novel recurrence formulas. This makes the implementation of the solution very simple. Since the infinite-summation can be truncated to about 65 terms and there is no need for any numerical integration, the solution is computationally very efficient. The input impedance has been calculated, and good agreement between theory and experiment has been obtained. In the experiment, adhesive conducting tapes were used to remove the air gap between the DRA and the ground plane. The technique has led to a substantial improvement in the impedance measurement. The effects of the strip length and dielectric constant on the input impedance have been studied. It has been observed that the effects are similar to those in the probe-feed case. Finally, The radiation patterns of the broadside TE_{111} mode have been presented. It has been found that because of having no $\hat{r}$-directed current components, the cross-polarized field is much weaker than in the probe-feed case, as desired.

Acknowledgment

The author would like to thank K. Y. Chow and W. C. Wong for their valuable help in the measurement process.

References

[1] S. A. Long, M. W. McAllister, and L. C. Shen, "The resonant cylindrical dielectric cavity antenna," *IEEE Trans. Antennas Propagat.*, vol. AP-31, pp. 406–412, May 1983.

[2] M. W. McAllister, S. A. Long, and G. L. Conway, "Rectangular dielectric resonator antenna," *Electron. Lett.*, vol. 19, pp. 218–219, Mar. 1983.

[3] M. W. McAllister and S. A. Long, “Resonant hemispherical dielectric antenna,” *Electron. Lett.*, vol. 20, pp. 657–659, Aug. 1984.
[4] K. W. Leung, K. M. Luk, K. Y. A. Lai, and D. Lin, “Theory and experiment of a coaxial probe fed dielectric resonator antenna,” *IEEE Trans. Antennas Propagat.*, vol. 41, pp. 1390–1398, Oct. 1993.
[5] G. P. Junker, A. A. Kishk, and A. W. Glisson, “Input impedance of dielectric resonator antennas excited by a coaxial probe,” *IEEE Trans. Antennas Propagat.*, vol. 42, pp. 960–966, July 1994.
[6] K. L. Wong, N. C. Chen, and H. T. Chen, “Analysis of a hemisphere dielectric resonator antenna with an airgap,” *IEEE Microwave Guided Wave Lett.*, vol. 3, pp. 355–357, Oct. 1993.
[7] S. M. Shum and K. M. Luk, “FDTD analysis of probe-fed cylindrical dielectric resonator antenna,” *IEEE Trans. Antennas Propagat.*, vol. 46, pp. 325–333, Mar. 1998.
[8] J. T. H. St. Martin, Y. M. M. Antar, A. A. Kishk, and A. Ittipiboon, “Dielectric resonator antenna using aperture coupling,” *Electron. Lett.*, vol. 26, pp. 2015–2016, Nov. 1990.
[9] K. W. Leung, K. M. Luk, K. Y. A. Lai, and D. Lin, “Theory and experiment of an aperture-coupled hemispherical dielectric resonator antenna,” *IEEE Trans. Antennas Propagat.*, vol. 43, pp. 1192–1198, Nov. 1995.
[10] G. P. Junker, A. A. Kishk, and A. W. Glisson, “Input impedance of aperture-coupled dielectric resonator antennas,” *IEEE Trans. Antennas Propagat.*, vol. 44, pp. 600–607, May 1996.
[11] Y. M. M. Antar and Z. Fan, “Theoretical investigation of aperture-coupled rectangular dielectric resonator,” *Inst. Elect. Eng. Proc. Microwave Antennas Propagat.*, vol. 143, pp. 113–118, Apr. 1996.
[12] R. K. Mongia, A. Ittipiboon, Y. M. M. Antar, P. Bhartia, and M. Cuhaci, “A half-split cylindrical dielectric resonator antenna using slot-coupling,” *IEEE Microwave Guided Wave Lett.*, vol. 3, pp. 38–339, Feb. 1993.
[13] N. C. Chen, K. L. Wong, and K. W. Leung, “Input impedance of inclined printed slot antennas and inclined-slot-coupled dielectric resonator antennas,” *Microwave Opt. Technol. Lett.*, vol. 12, pp. 47–50, May 1996.
[14] R. A. Kranenburg and S. A. Long, “Microstrip transmission line excitation of dielectric resonator antennas,” *Electron. Lett.*, vol. 24, pp. 1156–1157, Sept. 1988.
[15] K. W. Leung, K. Y. Chow, K. M. Luk, and E. K. N. Yung, “Low-profile circular disk DR antenna of very high permittivity excited by a microstripline,” *Electron. Lett.*, vol. 33, pp. 1004–1005, June 1997.
[16] R. A. Kranenburg, S. A. Long, and J. T. Williams, “Coplanar waveguide excitation of dielectric resonator antennas,” *IEEE Trans. Antennas Propagat.*, vol. 39, pp. 119–122, Jan. 1991.
[17] K. W. Leung, K. Y. Chow, K. M. Luk, and E. K. N. Yung, “Excitation of dielectric resonator antenna using a soldered-through probe,” *Electron. Lett.*, vol. 33, pp. 349–350, Feb. 1997.
[18] K. W. Leung and M. W. To, “Aperture-coupled dielectric resonator antenna with a perpendicular feed,” *Electron. Lett.*, vol. 33, no. 12, pp. 1000–1001, June 1997.
[19] K. W. Leung, “Analysis of aperture-coupled hemispherical dielectric resonator antenna with a perpendicular feed,” *IEEE Trans. Antennas Propagat.*, pp. XXX–XXX, June 2000.
[20] G. P. Junker, A. A. Kishk, A. W. Glisson, and D. Kajfez, “Effect of fabrication imperfections for ground-plane-backed dielectric resonator antennas,” *IEEE Antennas Propagat. Mag.*, vol. 37, no. 1, pp. 40–46, 1995.
[21] R. K. Mongia, A. Ittipiboon, M. Cuhaci, and D. Roscoe, “Circularly polarized dielectric resonator antenna,” *Electron. Lett.*, vol. 30, pp. 1361–1362, Aug. 1994.
[22] G. Drossos, Z. Wu, and L. E. Davis, “Circular polarized cylindrical dielectric resonator antenna,” *Electron. Lett.*, vol. 32, pp. 281–283, Feb. 1996.
[23] K. W. Leung, K. K. Tse, K. M. Luk, and E. K. N. Yung, “Cross-polarization characteristics of a probe-fed hemispherical dielectric resonator antenna,” *IEEE Trans. Antennas Propagat.*, vol. 47, pp. 1228–1230, July 1999.
[24] A. A. Kishk, G. Zhou, and A. W. Glisson, “Analysis of dielectric-resonator antennas with emphasis on hemispherical structures,” *IEEE Antennas Propagat. Mag.*, vol. 36, pp. 20–31, Apr. 1994.
[25] R. F. Harrington, *Time-Harmonic Electromagnetic Fields.*. New York: McGraw-Hill, 1961.
[26] K. W. Leung, “Theory and experiment of a rectangular slot on a sphere,” *IEEE Trans. Microwave Theory Tech.*, vol. 46, pp. 2117–2123, Dec. 1998.

Kwok Wa Leung (S’90-M’93) was born in Hong Kong on April 11, 1967. He received the B.Sc. (electronics) and Ph.D. (electronic engineering) degrees from the Chinese University of Hong Kong, in 1990 and 1993, respectively.

From 1990 to 1993, he was a Graduate Assistant in the Department of Electronic Engineering, Chinese University of Hong Kong. He joined the Department of Electronic Engineering, City University of Hong Kong, as an Assistant Professor in 1994 and became an Associate Professor in 1999. His research interests include dielectric resonator antennas, microstrip antennas, wire antennas, numerical methods in electromagnetics, and mobile communications.